

# *NLK* interacts with 14-3-3 $\zeta$ to restore the expression of E-cadherin

JIE CHEN<sup>1\*</sup>, QINGFENG LIN<sup>1\*</sup>, TINGTING NI<sup>2\*</sup>, JIYI ZHAO<sup>3</sup>, FENG LIN<sup>1</sup>, XIANGDONG LU<sup>1</sup>, YE LV<sup>1</sup>, SHUJUAN REN<sup>1</sup>, ZHILI LIU<sup>1</sup>, TING ZHANG<sup>4</sup>, SHUYAN HE<sup>1</sup>, DONG SHEN<sup>1</sup> and WEIDONG MAO<sup>1</sup>

<sup>1</sup>Department of Oncology, The Jiangyin Clinical College of Xuzhou Medical University, Wuxi, Jiangsu 214400;

<sup>2</sup>Department of Oncology, Nantong Tumor Hospital, Nantong, Jiangsu 226001; Departments of <sup>3</sup>Gastroenterology and

<sup>4</sup>Central Laboratory, The Jiangyin Clinical College of XuZhou Medical University, Wuxi, Jiangsu 214400, P.R. China

Received September 3, 2019; Accepted February 28, 2020

DOI: 10.3892/or.2020.7557

**Abstract.** The Nemo-like kinase (*NLK*), a conserved serine/threonine kinase, plays a critical role in the regulation of a variety of transcription factors, with important roles in determining cell fate. Although recent studies have demonstrated decreased expression patterns of *NLK* in various types of human cancer, the functional mechanism of *NLK* in cancer development has not been elucidated. Here, in the present study overexpression of *NLK* was found to inhibit the growth and migration of the non-small cell lung cancer A549 cell line. *NLK* was subsequently found to interact with 14-3-3 $\zeta$  (also known as *YWHAZ*), which is responsible for E-cadherin silencing during epithelial-mesenchymal transition (EMT). Furthermore, *NLK* overexpression was able to restore the expression of E-cadherin inhibited by 14-3-3 $\zeta$ . Notably, *NLK* interacts with 14-3-3 $\zeta$  and prevents its dimerization, which is essential for 14-3-3 $\zeta$  stability and function. By fusing two copies of the 14-3-3 $\zeta$  gene, via a Gly-rich linker, a non-dissociable dimer of 14-3-3 $\zeta$  was formed. It was found that *NLK* was unable to restore the expression of E-cadherin inhibited by the overexpression of the fused dimer of 14-3-3 $\zeta$ . In addition, the increased ability of migration induced by the overexpression of fused 14-3-3 $\zeta$  dimer could not be altered by *NLK* overexpression. The results from the present study indicate that *NLK* is a negative regulator of 14-3-3 $\zeta$  and plays a tumor suppressive role in the inhibition of cancer cell migration.

## Introduction

Nemo-like kinase (*NLK*) is a conserved serine/threonine kinase and is involved in a variety of biological responses and is regulated by a variety of different transcription factors (1,2). Decreased expression of *NLK* was found in various types of human cancers. In human melanoma, decreased expression of *NLK* is associated with poor prognosis and increased vascularity, and metastasis (3). Decreased expression of *NLK* in human ovarian carcinomas is associated with poor patient survival (4,5). In addition, *NLK* is significantly downregulated in breast cancer tissues and non-small cell lung cancer (NSCLC) compared with that in corresponding normal tissues (6,7). *NLK* has also been identified as a tumor-suppressor gene in glioblastoma using an *in vivo* RNAi screen (8).

Epithelial-mesenchymal transition (EMT) is a biological process, involving the functional transition of polarized epithelial cells into mesenchymal cells, and is involved in cancer metastasis, migration, invasion, and progression (9-11). E-cadherin is typically repressed during EMT. Thus, E-cadherin is considered to be a suppressor of migration and invasion of malignant epithelial cancers (12,13). 14-3-3 $\zeta$  (also known as *YWHAZ*) is a member of the evolutionally conserved regulatory family that mediates signal transduction by binding to phosphoserine-containing proteins (14). 14-3-3 $\zeta$  was found to be responsible for silencing of E-cadherin during EMT (15).

In the present study, overexpression of *NLK* was found to inhibit the growth and migration of the NSCLC A549 cell line. Moreover, *NLK* interacts with 14-3-3 $\zeta$  and prevents its dimerization. In addition, *NLK* overexpression was able to restore the expression of E-cadherin inhibited by 14-3-3 $\zeta$  but not with the fused dimer of 14-3-3 $\zeta$ . The results from the present study demonstrate that *NLK* is a negative regulator of 14-3-3 $\zeta$  and plays a tumor-suppressive role by inhibiting the migration of cancer cells.

## Materials and methods

**Cell culture.** The human A549, H358, H322, H23, H1437, H1650, Calu-3 and H441 lung cancer epithelial cell lines and human 293T cells were obtained from the Chinese Academy of Sciences cell bank, and were cultured in DMEM

---

**Correspondence to:** Professor Dong Shen or Professor Weidong Mao, Department of Oncology, The Jiangyin Clinical College of Xuzhou Medical University, Wuxi, Jiangsu 214400, P.R. China  
E-mail: sdshendong@126.com  
E-mail: maoweidongjy@126.com

\*Contributed equally

**Key words:** *NLK*, 14-3-3 $\zeta$ , E-cadherin, epithelial-to-mesenchymal transition, EMT

(cat no. 10-013-CV; Corning, Inc.) containing 10% FBS (cat no. 35-010-CV; Corning, Inc.), 100 U/ml penicillin and 100 mg/ml streptomycin at 37°C in a 95% humidified incubator with 5% CO<sub>2</sub>.

**Antibodies.** Rabbit antibodies to 14-3-3 $\zeta$  (cat. no. ab155037; dilution 1:1,000) and  $\beta$ -actin (cat. no. ab227387; dilution 1:2,000) were obtained from Abcam. Rabbit antibodies to *NLK* (cat. no. 94350; dilution 1:500), E-cadherin (cat. no. 3195; dilution 1:500) and HA tag (cat. no. 3724; dilution 1:2,000) were purchased from Cell Signaling Technology, Inc. Mouse antibodies to FLAG-M2 tag (cat. no. F1804; dilution 1:2,000), FLAG-M2 affinity gel (cat. no. A2220) and HA affinity gel (cat. no. A2095) were purchased from Sigma-Aldrich (Merck KGaA). Horseradish peroxidase (HRP)-linked anti-mouse IgG (cat. no. 7076; dilution 1:5,000) and anti-rabbit IgG (cat. no. 7074; dilution 1:5,000) were purchased from Cell Signaling Technology, Inc. HRP-linked light chain specific goat anti-mouse IgG (cat. no. 115-005-174) and mouse anti-rabbit IgG (cat. no. 211-002-171) for immunoprecipitation (IP) were purchased from Jackson ImmunoResearch Laboratories, Inc.

**Lentivirus packaging and transduction.** The lentivirus pCDH vector containing *NLK*, C-terminal FLAG tagged *NLK*, 14-3-3 $\zeta$ , C-terminal FLAG/HA tagged 14-3-3 $\zeta$ , 14-3-3 $\zeta$ -Fusion [by a 10-amino acid Glycine (Gly)-rich linker] and FLAG tagged 14-3-3 $\zeta$ -Fusion were purchased from Genesent Biological Technology Co., Ltd. To prepare the lentivirus, 293T cells were transfected with the aforementioned lentiviral vectors and packaging plasmids using Lipofectamine<sup>®</sup> 3000 (Thermo Fisher Scientific, Inc.) according to the manufacturer's instructions. Virus-containing medium was collected 48 h after transfection and filtered through 0.45  $\mu$ M low protein-binding filters (Nalgene; Thermo Fisher Scientific, Inc.). For transduction, cells were infected with lentiviral vectors and selected with puromycin. Subsequently, the expression levels of the target genes were detected using western blot analysis.

**Colony formation assay.** For colony formation, A549 cells were seeded in 6-well plates at 500 cells per well, and cultured for 2 weeks. When clones were visible, the colonies were fixed with 4% paraformaldehyde for 30 min and stained with 0.1% crystal violet (Sigma-Aldrich; Merck KGaA) for 5 min. Subsequently images of the cells were obtained and the number of cells were counted under an Olympus BX51 fluorescence microscope (magnification x100; Olympus Corp.).

**Wound healing assay.** Total 5x10<sup>5</sup> A549 cells infected with different lentivirus were cultured using 6-well plates. After cells had grown to produce a 90% confluent monolayer, a pipette tip (200  $\mu$ l) was used to create a wound. The cells were washed twice with PBS to remove non-adherent cells and cultured in serum-free medium for 18 or 24 h. Subsequently, the images of wound healing were obtained an Olympus BX51 fluorescence microscope (magnification x100; Olympus Corp.) and the migration rate was calculated. The migration rate was calculated using the following formula: Migration rate=(Area of original wound - Area of actual wound)/Area of original wound x100%.

**Sphere formation assay.** Monolayer cultured A549 cells (1,000 cells per well) infected with different lentivirus were suspended in 24-well ultra-low attachment plates (Corning, Inc.) with serum-free DMEM/F12 containing 20 ng/ml of epidermal growth factor (Thermo Fisher Scientific, Inc.), 20 ng/ml of basic fibroblast growth factor (Sigma-Aldrich; Merck KGaA) and 2% B27 supplement (Thermo Fisher Scientific, Inc.). After 7 days of incubation, images of the spheres were obtained under a phase-contrast Olympus BX51 microscope (magnification x100; Olympus Corp.).

**IP and liquid chromatography-mass spectrometry (LC-MS)/MS analysis.** For the IP assay, cells were harvested and lysed with RIPA buffer [50 mM Tris-HCl (pH7.4), 150 mM NaCl, 1.0% NP-40, and 0.25% sodium deoxycholate] with protease inhibitor and phosphatase inhibitor cocktail (Roche Diagnostics, GmbH). Following brief sonication, the lysates were centrifuged at 15,000 x g for 15 min at 4°C and the supernatants were subsequently incubated with the indicated primary antibodies together with protein A/G-sepharose beads (Santa Cruz Biotechnology, Inc.) or direct with FLAG-M2 affinity gel at 4°C for 2 h. The beads were washed three times before heating or adding FLAG peptides (Sigma-Aldrich; Merck KGaA). Isolated protein, including *NLK*-FLAG and its associated proteins were forwarded to Taiyuan Rosetta Stone Biotech Co., Ltd. for LC-MS/MS analysis. The mass of the peptides was identified using LTQ-XL mass spectrometer (Thermo Fisher Scientific, Inc.).

**SDS-PAGE and western blot analysis.** Total proteins were lysed with RIPA lysis buffer (cat. no. 9806; Cell Signaling Technology, Inc.). For denaturing conditions, the cell lysates were mixed with 5X SDS denaturing sample buffer (cat. no. 39000; Thermo Fisher Scientific, Inc.), and incubated at 95°C for 5 min. For non-denaturing conditions, the cell lysates were mixed with 2X SDS non-denaturing sample buffer (cat. no. LC2673; Thermo Fisher Scientific, Inc.) without 2-mercaptoethanol and incubated at room temperature for 60 min. The protein was separated using 12% SDS-PAGE or NativePAGE<sup>™</sup> (Thermo Fisher Scientific, Inc.), and subsequently transferred onto a PVDF membrane (EMD Millipore; Merck KGaA). The PVDF membranes were blocked in 5% skimmed milk for 1 h at room temperature, and incubated with aforementioned primary antibodies overnight at 4°C. Following which, the membranes were washed with TBS-Tween-20 and incubated with the aforementioned secondary antibodies for 1 h at room temperature. Proteins were visualized using enhanced chemiluminescence reagents (Roche Diagnostics GmbH). Densitometric analysis was performed using ImageJ software (version 1.48; National Institutes of Health).

**Statistical analysis.** GraphPad Prism 5 software (GraphPad Software, Inc.) was used to analyze the data. Data are presented as the mean  $\pm$  standard deviation. All experiments were repeated 3 times. Two-tailed Student's t-test was used when two independent groups were compared, while one-way analysis of variance (ANOVA) followed by Tukey's multiple comparison was used for multiple comparison tests. A P<0.05 was considered to indicate a statistically significant difference.

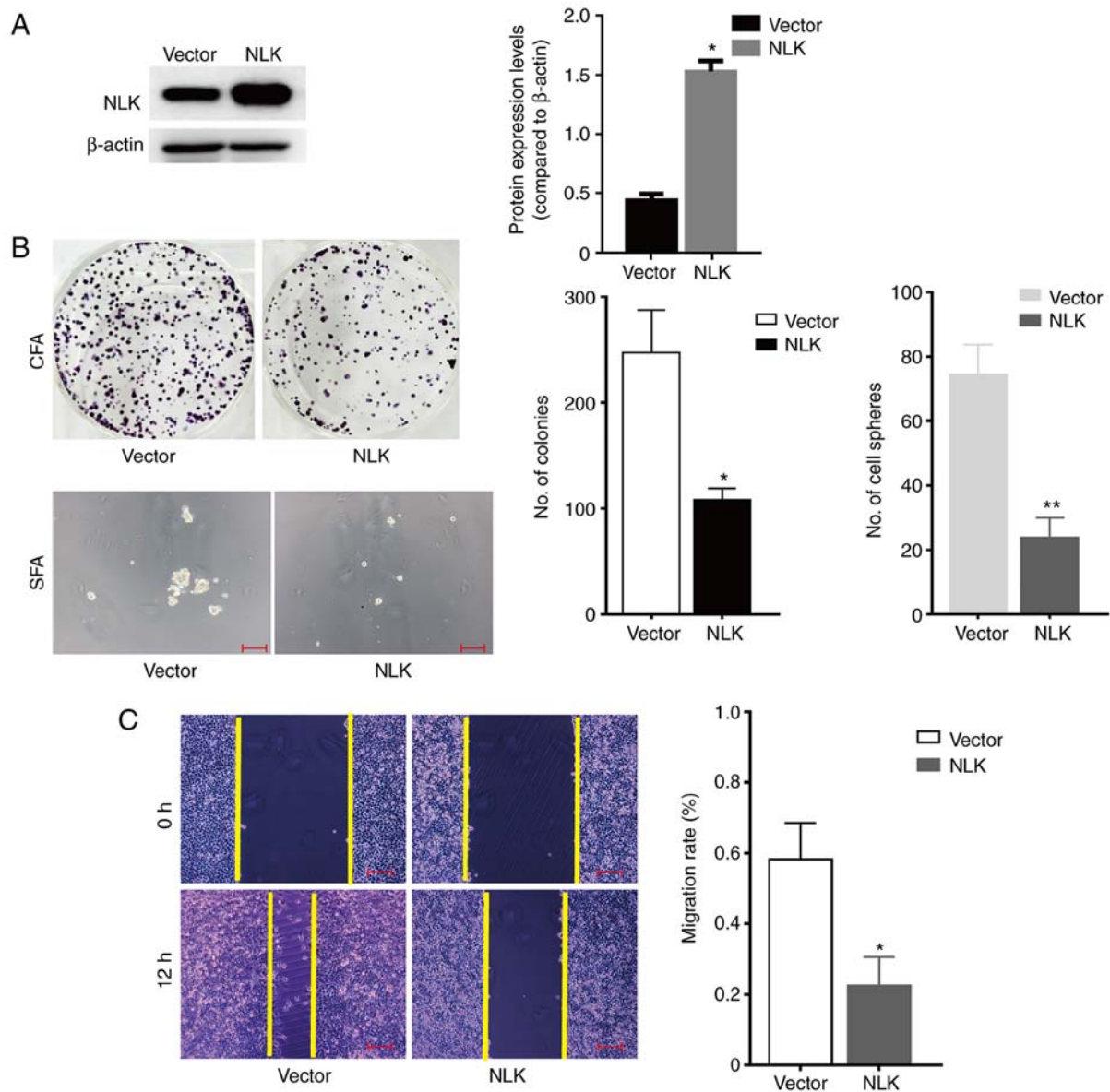


Figure 1. *NLK* inhibits the cell growth and migration of A549 cells. (A) Western blot analysis of *NLK* protein expression in A549 cells transfected with the *NLK* lentivirus or vector lentivirus; Densitometric analysis of the relative expression level of *NLK*. \* $P < 0.001$  compared to the Vector group. (B) Colony formation assay (CFA): Representative images and quantification of the colony formation of A549 cells transfected with *NLK* or vector lentivirus. \* $P < 0.01$  compared to the Vector group. Sphere formation assay (SFA): The spheres were derived from A549 cells transfected with *NLK* lentivirus or vector lentivirus. \*\* $P < 0.001$  compared to the Vector group (scale bar, 200  $\mu\text{m}$ ). (C) Wound healing assay indicated that *NLK* overexpression suppressed A549 cell migration. \* $P < 0.01$  compared to the Vector group (scale bar, 200  $\mu\text{m}$ ). *NLK*, nemo-like kinase.

## Results

***NLK* inhibits cell growth and migration.** To examine whether overexpression of *NLK* affects cell growth, lentivirus transfection was used to upregulate the gene expression of *NLK* in A549 cells. From the western blot analysis, A549 cells showed stable overexpression of *NLK* compared with that in the control cells transfected with the vector only (Fig. 1A). Colony formation assay (CFA) demonstrated that overexpression of *NLK* significantly represses colony formation ability, and overexpression of *NLK* significantly repressed sphere formation capabilities (SFA) in the A549 cells (Fig. 1B). Wound healing assay was used to determine whether overexpression of *NLK* affected the migration ability of A549 cells, and it was found that overexpression of *NLK* resulted in significantly decreased

migration of A549 cells compared with that in cells transfected with the vector only (Fig. 1C). The results suggest that *NLK* significantly inhibited cell growth and migration capabilities.

***NLK* interacts with 14-3-3 $\zeta$ .** To further understand the mechanism of *NLK* in the regulation of cell growth and migration, IP and MS analyses were used to identify *NLK* binding proteins in A549 cells stably expressing C-terminally FLAG-tagged *NLK* (*NLK*-FLAG) created using lentivirus transfection. Cell extracts were subjected to IP with FLAG agarose beads. The specific bands of *NLK*-FLAG in isolated proteins were identified using western blot analysis (Fig. 2A). Subsequently, the isolated proteins, including *NLK*-FLAG and its associated proteins were analyzed using LC-MS/MS to identify *NLK*-interacting proteins. The tryptic peptides

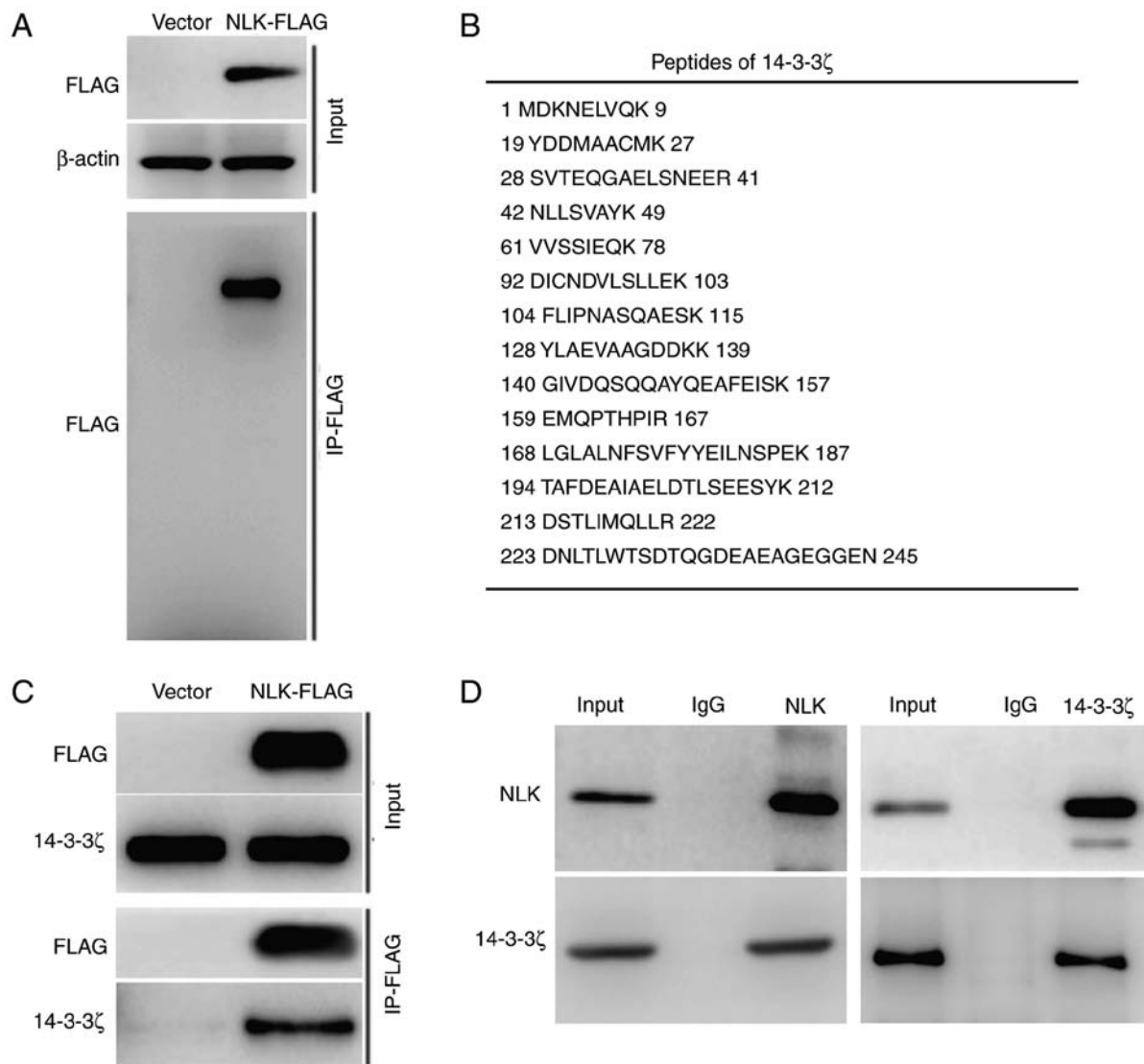


Figure 2. Association of *NLK* with 14-3-3 $\zeta$ . (A) A549 cells expressing FLAG-tagged *NLK* were lysed and immunoprecipitation (IP) was performed by FLAG-M2 Affinity Gel. Immunoprecipitated protein was subjected to western blot and detected by FLAG antibody. (B) List of 14-3-3 $\zeta$  peptides identified by LC-MS/MS. (C) Immunoprecipitated *NLK*-FLAG associated protein in A549 cells was subjected to western blot analysis by 14-3-3 $\zeta$  antibody. (D) A549 cells were lysed and subjected to IP with *NLK* or 14-3-3 $\zeta$  antibodies, controlled by corresponding IgG. Immunoprecipitated protein were then analyzed by western blot analysis. *NLK*, nemo-like kinase; LC-MS/MS, liquid chromatography with tandem mass spectrometry.

corresponding to 14-3-3 $\zeta$  protein with a high sequence coverage were identified (Fig. 2B). The interaction between *NLK*-FLAG and 14-3-3 $\zeta$  was further verified using western blot analysis with the precipitated proteins (Fig. 2C). Moreover, endogenous *NLK* and 14-3-3 $\zeta$  also showed an interaction in A549 cells (Fig. 2D). These data indicate that 14-3-3 $\zeta$  is a novel *NLK*-interacting protein.

*NLK* inhibits the dimerization of 14-3-3 $\zeta$  and restores 14-3-3 $\zeta$ -repressed *E-cadherin* expression. A previous study has shown that 14-3-3 $\zeta$  is responsible for silencing of *E-cadherin* during EMT (15). Lentivirus transfection was used to upregulate the gene expression of 14-3-3 $\zeta$  in A549 cells (Fig. 3A). It was subsequently confirmed that overexpression of 14-3-3 $\zeta$  induced a more spindle-like cell shape and a scattered distribution, suggesting decreased epithelial cell-to-cell contacts in the A549 cells (Fig. 3A). In addition, A549 cells stably overexpressing 14-3-3 $\zeta$  were transfected with the

*NLK* lentivirus to create *NLK*/14-3-3 $\zeta$  double-overexpressing cells. EMT morphological changes induced by 14-3-3 $\zeta$  overexpression were inhibited by *NLK* overexpression (Fig. 3A). Subsequently it was confirmed that overexpression of 14-3-3 $\zeta$  inhibited the expression of *E-cadherin* (Fig. 3B). Furthermore, *NLK*/14-3-3 $\zeta$  double-overexpressing cells revealed restored expression of *E-cadherin* compared with that in cells overexpressing 14-3-3 $\zeta$  (Fig. 3B). It has been reported that dimerization is essential for 14-3-3 $\zeta$  stability and the ability of 14-3-3 $\zeta$  to bind to its target proteins (16,17). Using non-denaturing conditions, which would preserve any disulfide linkages during western blot analysis, an endogenous 14-3-3 $\zeta$  dimer band was found in A549 cells (Fig. 3C). Moreover, the 14-3-3 $\zeta$  monomer band and 14-3-3 $\zeta$  dimer band were found to be increased in A549 cells stably overexpressing 14-3-3 $\zeta$ . On the other hand, the 14-3-3 $\zeta$  dimer band was inhibited in *NLK*/14-3-3 $\zeta$  double-overexpressing cells as compared with that in 14-3-3 $\zeta$  overexpressing cells (Fig. 3C).

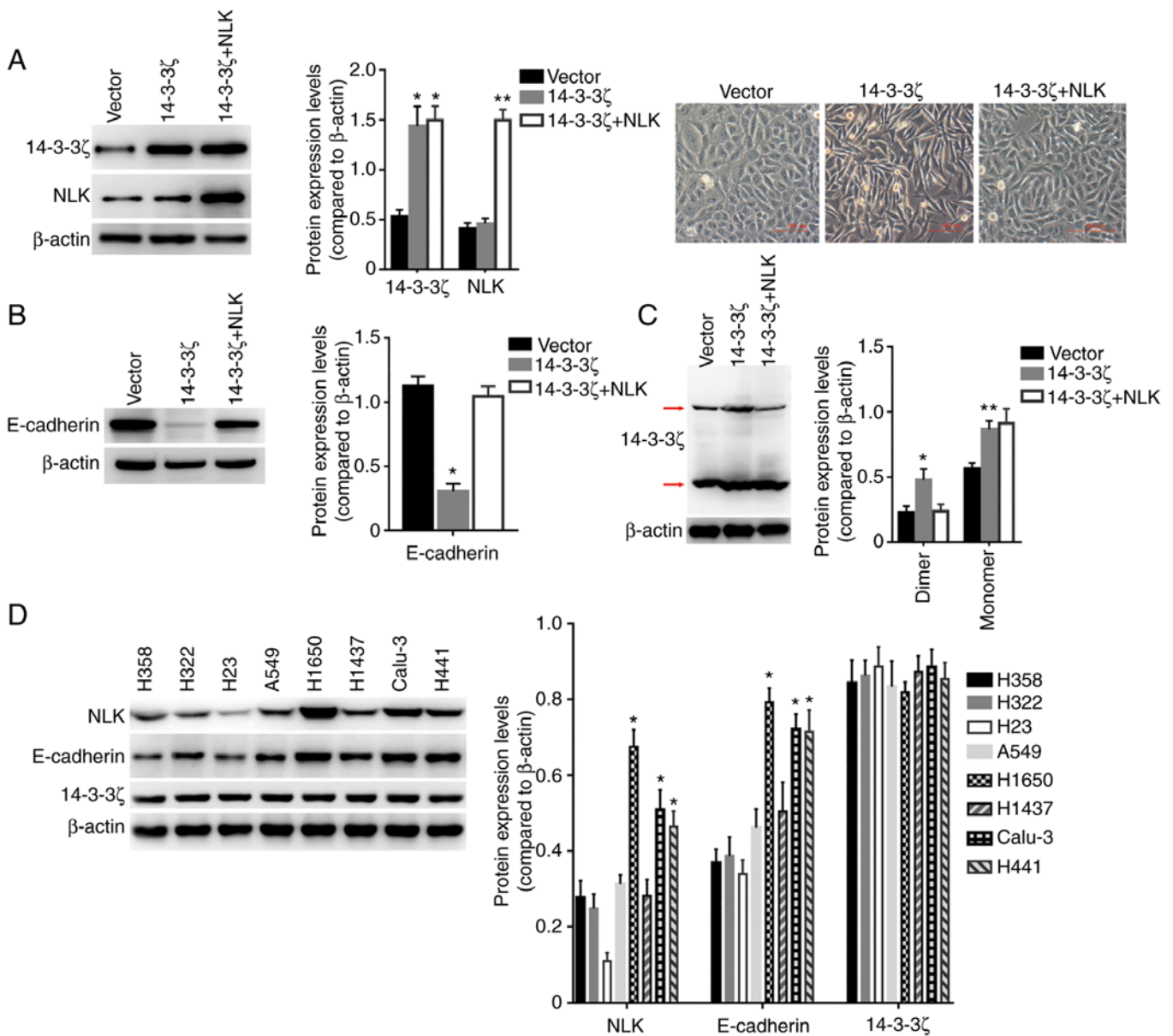


Figure 3. *NLK* regulates 14-3-3 $\zeta$ -repressed E-cadherin expression. (A) Left panels: Expression of *NLK*, 14-3-3 $\zeta$  and  $\beta$ -actin were detected by western blot in A549 cells transfected with the vector lentivirus, 14-3-3 $\zeta$  lentivirus or 14-3-3 $\zeta$  plus *NLK* lentivirus, and densitometric analysis of the relative expression levels of 14-3-3 $\zeta$  and *NLK*. \* $P < 0.001$  compared to the Vector group; \*\* $P < 0.001$  compared to the other groups. Right images: The cells exhibited different morphologies. (B) Expression of E-cadherin and  $\beta$ -actin were detected by western blot analysis in A549 cells transfected with the vector lentivirus, 14-3-3 $\zeta$  lentivirus or 14-3-3 $\zeta$  plus *NLK* lentivirus, and densitometric analysis of the relative expression level of E-cadherin. \* $P < 0.005$  compared to other groups. (C) Under non-denaturing condition, the expression of 14-3-3 $\zeta$  and  $\beta$ -actin were detected by western blot analysis in A549 cells transfected with the vector lentivirus, 14-3-3 $\zeta$  lentivirus or 14-3-3 $\zeta$  plus *NLK* lentivirus, and densitometric analysis of the relative expression levels of dimer and monomer of 14-3-3 $\zeta$ . \* $P < 0.01$  compared to other groups; \*\* $P < 0.05$  compared to the Vector group. (D) Expression of *NLK*, E-cadherin, 14-3-3 $\zeta$  and  $\beta$ -actin were detected by western blot analysis in 8 human lung cancer cell lines, and densitometric analysis of the relative expression levels of *NLK*, E-cadherin and 14-3-3 $\zeta$ . \* $P < 0.005$  compared to the other groups. *NLK*, nemo-like kinase.

At the protein level, expression of E-cadherin was evaluated in 8 human lung cancer cell lines using western blot analysis. There were no differences in the expression levels of 14-3-3 $\zeta$  in these cells, and the expression levels between *NLK* and E-cadherin were highly correlated (Fig. 3D). These results suggest that *NLK* may be involved in 14-3-3 $\zeta$ -regulated E-cadherin expression by the interaction with 14-3-3 $\zeta$ . Using lentivirus transfection, A549 cells stably sole-expressing or co-expressing FLAG-14-3-3 $\zeta$  and HA-14-3-3 $\zeta$  were generated. As shown in Fig. 4A, FLAG-14-3-3 $\zeta$  was co-immunoprecipitated with HA-14-3-3 $\zeta$  in FLAG-14-3-3 $\zeta$  and HA-14-3-3 $\zeta$  co-expressing A549 cells. Notably, overexpression of untagged

*NLK* in FLAG-14-3-3 $\zeta$  and HA-14-3-3 $\zeta$  co-expressing cells inhibited the interaction between FLAG-14-3-3 $\zeta$  and HA-14-3-3 $\zeta$  (Fig. 4B and C). These results suggest that *NLK* disturbs 14-3-3 $\zeta$ -14-3-3 $\zeta$  dimerization.

*NLK* regulation of E-cadherin expression depends on the homodimer of 14-3-3 $\zeta$ . Gly-rich linkers are flexible and naturally exist in a number of proteins of their Gly residues (18-20). Thus, Gly-rich linkers have been used to create fusion proteins with independent sequences, including the connection with the homodimer, ligand-receptor and co-activators (21-23). By fusing two copies of the 14-3-3 $\zeta$  gene via a 10-amino acid Gly-rich

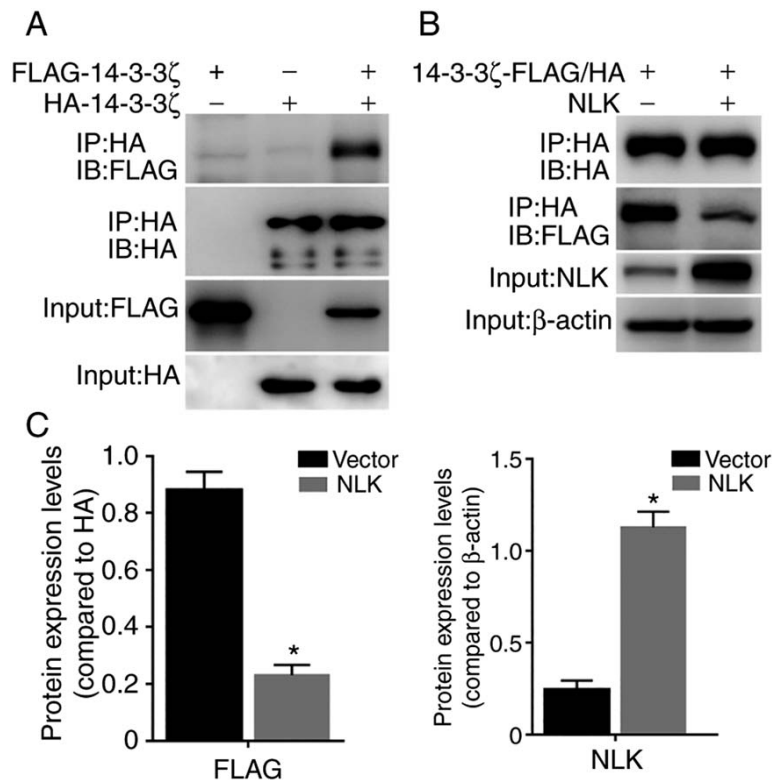


Figure 4. *NLK* inhibits the dimerization of 14-3-3 $\zeta$ . (A) A549 cells stably sole-expressing or co-expressing FLAG-14-3-3 $\zeta$  and HA-14-3-3 $\zeta$ . Cell lysates was immunoprecipitated with HA Affinity Gel and subjected to western blot analysis as detected by the FLAG or HA antibody. (B) A549 cells co-expressing FLAG-14-3-3 $\zeta$  and HA-14-3-3 $\zeta$  were transfected with the vector lentivirus or untagged *NLK* lentivirus. Cell lysates was immunoprecipitated with HA Affinity Gel and subjected to western blot analysis. (C) Densitometric analysis of the relative expression level of untagged *NLK* and FLAG-tagged 14-3-3 $\zeta$  associated with equal amounts of HA-tagged 14-3-3 $\zeta$ . \* $P$ <0.001 compared to Vector group. *NLK*, nemo-like kinase.

linker, a non-dissociable dimer of 14-3-3 $\zeta$  (14-3-3 $\zeta$ -Fusion) with lentiviral vector (Fig. 5A) was generated. As shown in Fig. 5A, the expression of the fused dimer of 14-3-3 $\zeta$  and endogenous 14-3-3 $\zeta$  were examined using western blot analysis, under denaturing and non-denaturing conditions.

Moreover, spindle-like cell shape and a scattered distribution were also found in cells stably expressing 14-3-3 $\zeta$ -Fusion. The EMT morphological changes were not inhibited by overexpression of *NLK* (Fig. 5A). Meanwhile, 14-3-3 $\zeta$ -repressed E-cadherin expression could not be restored by *NLK* overexpression (Fig. 5B).

To further determine whether *NLK* binds to the monomer or dimer form of 14-3-3 $\zeta$ , the endogenous interaction between *NLK* and 14-3-3 $\zeta$  under non-denaturing conditions was investigated. As shown in Fig. 5C, *NLK* was found to be associated with the monomer form but not with the dimer form of 14-3-3 $\zeta$  under non-denaturing conditions. Moreover, exogenous FLAG-tagged 14-3-3 $\zeta$  dimer fusion protein (14-3-3 $\zeta$ -Fusion-FLAG) could not bind to endogenous *NLK* in 14-3-3 $\zeta$ -Fusion-FLAG expressing cells (Fig. 5C). In addition, wound healing assay revealed that 14-3-3 $\zeta$  overexpression enhanced the migration of A549 cells. *NLK* was able to inhibit the increased migration from 14-3-3 $\zeta$  overexpression. On the other hand, 14-3-3 $\zeta$ -Fusion overexpression revealed a higher migration ability compared with that in 14-3-3 $\zeta$ -overexpressing cells and this effect was not regulated by *NLK* (Fig. 5D). Together, these results suggest that *NLK* regulation of E-cadherin expression depends on the homodimer of 14-3-3 $\zeta$ .

## Discussion

EMT is involved in cancer metastasis, migration, invasion, and progression. E-cadherin is essential for the maintenance of intercellular adhesion as a key component of the adherens junctions (24). Thus, the loss of E-cadherin is considered to be a major hallmark of EMT and has been reported in various types of cancers (25). 14-3-3 $\zeta$ , a member of the evolutionally conserved family, mediates signal transduction by binding to phosphoserine-containing proteins. Dimerization is essential for 14-3-3 $\zeta$  stability and the ability of 14-3-3 $\zeta$  to bind its target proteins (16). 14-3-3 $\zeta$  was found to be responsible for silencing of E-cadherin during EMT (15). In the present study, a novel *NLK*-interacting protein was identified. *NLK* was found to inhibit cell growth capabilities using colony formation assay. The number or size of spheres partly reveals the proliferation of cancer stem/progenitor cells (26). The sphere formation assay revealed that *NLK* markedly repressed the sphere formation capacities in A549 cells, in the present study. Furthermore, wound healing assay was performed to examine the effect of *NLK* on migration ability. Overexpression of *NLK* markedly inhibited cell migration. As an *NLK*-interacting protein, 14-3-3 $\zeta$  overexpressing cells revealed enhanced migration capacity. *NLK* and 14-3-3 $\zeta$  co-expressing cells revealed decreased migration compared with that in cells only expressing 14-3-3 $\zeta$ . These findings suggest that *NLK* inhibition of migration may be dependent on the regulation of 14-3-3 $\zeta$  function.

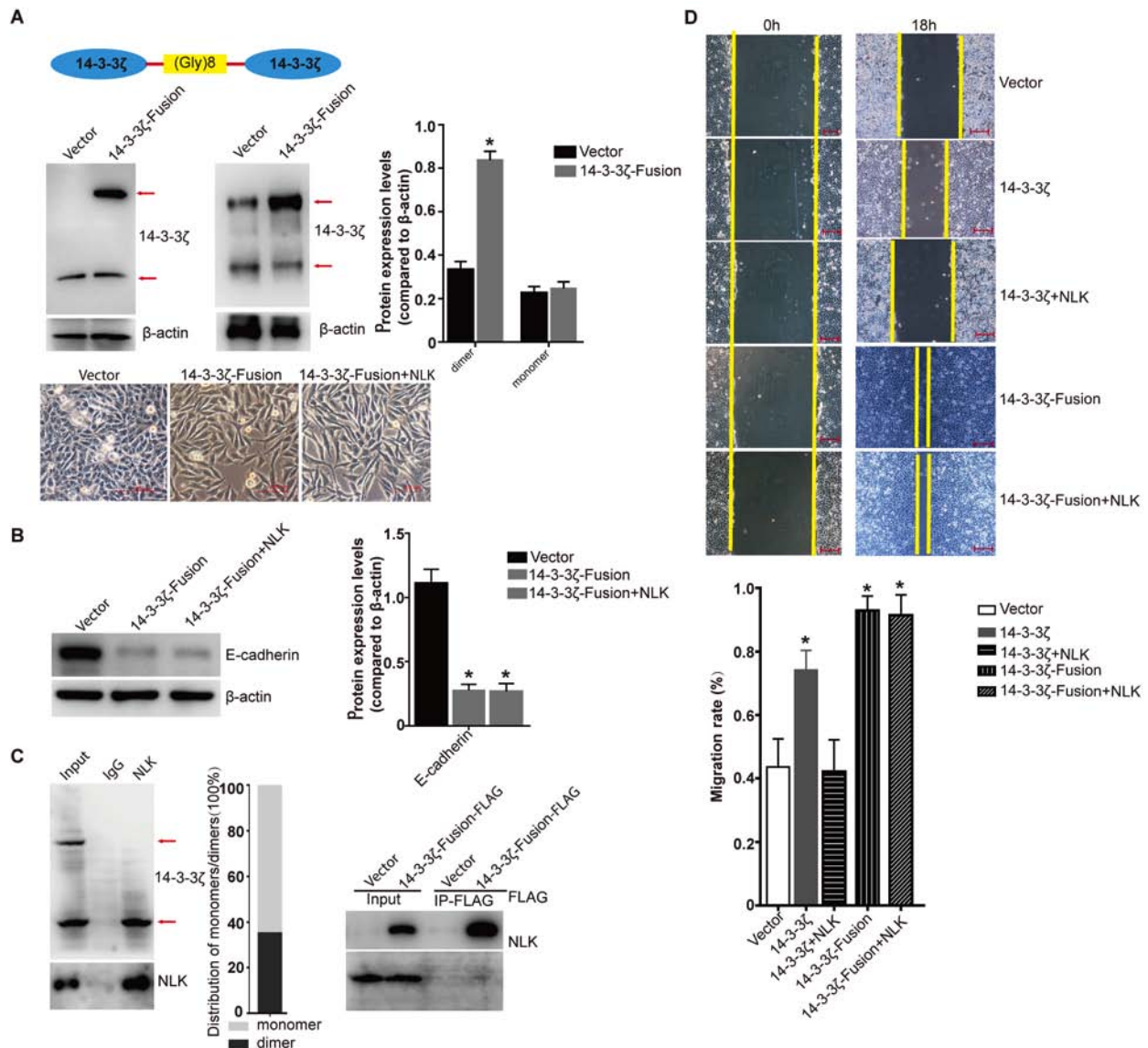


**Figure 5.** The function of non-dissociable homodimer of 14-3-3 $\zeta$ . (A) Two copies of the 14-3-3 $\zeta$  gene via a 10-amino acid Gly-rich linker to get a non-dissociable dimer of 14-3-3 $\zeta$  (14-3-3 $\zeta$ -Fusion) with lentiviral vector. Expression of endogenous 14-3-3 $\zeta$  and 14-3-3 $\zeta$ -Fusion was detected by western blot analysis in A549 cells transfected with the vector and 14-3-3 $\zeta$ -Fusion lentivirus (left: Under denaturing condition, right: Under non-denaturing condition). Densitometric analysis of the relative expression level of dimer and monomer of 14-3-3 $\zeta$ . \* $P$ <0.005 compared to the Vector group. Lower images: The cells exhibited different morphologies with the transfection of the vector, 14-3-3 $\zeta$ -Fusion or 14-3-3 $\zeta$ -Fusion plus untagged *NLK* lentivirus (scale bar, 100  $\mu$ m). (B) Expression of E-cadherin and  $\beta$ -actin was detected by western blot analysis in A549 cells transfected with the vector lentivirus, 14-3-3 $\zeta$ -Fusion or 14-3-3 $\zeta$ -Fusion plus untagged *NLK* lentivirus. Densitometric analysis of the relative expression level of E-cadherin. \* $P$ <0.001 compared to the Vector group. (C) Left: A549 cells were lysed and subjected to IP with *NLK* antibodies, controlled by corresponding IgG. Immunoprecipitated protein were then analyzed by western blot analysis under non-denaturing condition. Right: Immunoprecipitated 14-3-3 $\zeta$ -Fusion-FLAG-associated protein in A549 cells was subjected to western blot analysis. (D) Wound healing analysis of A549 cells transfected with the vector, 14-3-3 $\zeta$ , 14-3-3 $\zeta$ -Fusion, 14-3-3 $\zeta$  plus *NLK* or 14-3-3 $\zeta$ -Fusion plus *NLK* lentivirus. \* $P$ <0.005 compared to the Vector or 14-3-3 $\zeta$ +*NLK* groups (scale bar, 200  $\mu$ m). *NLK*, nemo-like kinase; IP, immunoprecipitation.

14-3-3 $\zeta$  has been previously found to promote EMT and inhibit the expression of E-cadherin (15). In the present study, 14-3-3 $\zeta$  was found to induce EMT and repress E-cadherin in A549 cells. Co-immunoprecipitation assay was performed with exogenous tagged protein or endogenous proteins to verify the interaction between *NLK* and 14-3-3 $\zeta$  identified by LC-MS/MS analysis of *NLK*-interacting proteins. In light of the key role of *NLK* in the regulation of 14-3-3 $\zeta$ -induced E-cadherin repression, A549 cells stably co-expressing FLAG-14-3-3 $\zeta$  and HA-14-3-3 $\zeta$  were constructed. FLAG-14-3-3 $\zeta$  was found to be co-immunoprecipitated with HA-14-3-3 $\zeta$ . Notably, overexpression of untagged *NLK* in FLAG-14-3-3 $\zeta$  and HA-14-3-3 $\zeta$

co-expressing cells inhibits the interaction between FLAG-14-3-3 $\zeta$  and HA-14-3-3 $\zeta$ . These results suggest that *NLK* disturbs the 14-3-3 $\zeta$ -14-3-3 $\zeta$  dimerization, and hence the function of *NLK* to regulate E-cadherin.

Gly-rich linkers naturally exist in a number of proteins and have been used to create fusion proteins with independent sequences, such as the connection with homodimer, ligand-receptor and co-activators (18). Overexpression of 14-3-3 $\zeta$ -Fusion created by Gly-rich linker successfully repressed the expression of E-cadherin, promoted EMT morphological changes and cell migration. Notably, *NLK* lost its ability to regulate the expression of E-cadherin,

EMT morphological changes and cell migration induced by 14-3-3 $\zeta$ -Fusion overexpression. In conclusion, the results from the present study reveals that *NLK* interacts with 14-3-3 $\zeta$  to represses the expression of E-cadherin by interrupting 14-3-3 $\zeta$  dimer formation.

### Acknowledgements

Not applicable.

### Funding

The present study was supported by the Scientific Research Youth Project of Wuxi Health and Family Planning Commission (Q201751).

### Availability of data and materials

The datasets used during the present study are available from the corresponding author upon reasonable request.

### Authors' contributions

JC, QL, TN, DS and WM conceived and designed the experiments. JC, QL and TN performed the majority of the experiments and assembled the data. JZ, FL, XL, YL, SR, ZL, TZ and SH participated in the other experiments and article revision. All authors read and approved the final manuscript and agree to be accountable for all aspects of the research in ensuring that the accuracy or integrity of any part of the work are appropriately investigated and resolved.

### Ethics approval and consent to participate

Not applicable.

### Patient consent for publication

Not applicable.

### Competing interests

The authors declare that they have no competing interests.

### References

- Huang Y, Yang Y, He Y and Li J: The emerging role of Nemo-like kinase (NLK) in the regulation of cancers. *Tumour Biol* 36: 9147-9152, 2015.
- Li SZ, Zhang HH, Liang JB, Song Y, Jin BX, Xing NN, Fan GC, Du RL and Zhang XD: Nemo-like kinase (NLK) negatively regulates NF- $\kappa$ B activity through disrupting the interaction of TAK1 with IKK $\beta$ . *Biochim Biophys Acta* 1843: 1365-1372, 2014.
- Yang Y, Zhe H, Massoumi R and Ke H: Decreased expression of nemo-like kinase in melanoma is correlated with increased vascularity and metastasis. *Melanoma Res* 29: 376-381, 2019.
- Stevens KN, Kelemen LE, Wang X, Fridley BL, Vierkant RA, Frederickson Z, Armasu SM, Tsai YY, Berchuck A, Narod SA, *et al*: Ovarian cancer association consortium: Common variation in Nemo-like kinase is associated with risk of ovarian cancer. *Cancer Epidemiol Biomarkers Prev* 21: 523-528, 2012.
- Zhang Y, Peng C, Wu G, Wang Y, Liu R, Yang S, He S, He F, Yuan Q, Huang Y, *et al*: Expression of NLK and its potential effect in ovarian cancer chemotherapy. *Int J Gynecol Cancer* 21: 1380-1387, 2011.
- Huang Y, Jiang Y, Lu W and Zhang Y: Nemo-like kinase associated with proliferation and apoptosis by c-Myb degradation in breast cancer. *PLoS One* 8: e69148, 2013.
- Ly L, Wan C, Chen B, Li M, Liu Y, Ni T, Yang Y, Liu Y, Cong X, Mao G and Xue Q: Nemo-like kinase (NLK) inhibits the progression of NSCLC via negatively modulating WNT signaling pathway. *J Cell Biochem* 115: 81-92, 2014.
- Sa JK, Yoon Y, Kim M, Kim Y, Cho HJ, Lee JK, Kim GS, Han S, Kim WJ, Shin YJ, *et al*: In vivo RNAi screen identifies NLK as a negative regulator of mesenchymal activity in glioblastoma. *Oncotarget* 6: 20145-20159, 2015.
- Campbell K, Rossi F, Adams J, Pitsidianaki I, Barriga FM, Garcia-Gerique L, Batlle E, Casanova J and Casali A: Collective cell migration and metastases induced by an epithelial-to-mesenchymal transition in *Drosophila* intestinal tumors. *Nat Commun* 10: 2311, 2019.
- Sjöberg E, Meyrath M, Milde L, Herrera M, Lövrot J, Hägerstrand D, Frings O, Bartish M, Rolny C, Sonnhhammer E, *et al*: A novel ACKR2-dependent role of fibroblast-derived CXCL14 in epithelial-to-mesenchymal transition and metastasis of breast cancer. *Clin Cancer Res* 25: 3702-3717, 2019.
- Zhang J, Shao S, Han D, Xu Y, Jiao D, Wu J, Yang F, Ge Y, Shi S, Li Y, *et al*: High mobility group box 1 promotes the epithelial-to-mesenchymal transition in prostate cancer PC3 cells via the RAGE/NF- $\kappa$ B signaling pathway. *Int J Oncol* 53: 659-671, 2018.
- Dong C, Yuan T, Wu Y, Wang Y, Fan TW, Miriyala S, Lin Y, Yao J, Shi J, Kang T, *et al*: Loss of FBP1 by Snail-mediated repression provides metabolic advantages in basal-like breast cancer. *Cancer Cell* 23: 316-331, 2013.
- Qi M, Zhou Y, Liu J, Ou X, Li M, Long X, Ye J and Yu G: AngII induces HepG2 cells to activate epithelial-mesenchymal transition. *Exp Ther Med* 16: 3471-3477, 2018.
- Guo F, Gao Y, Sui G, Jiao D, Sun L, Fu Q and Jin C: miR-375-3p/YWHAZ/ $\beta$ -catenin axis regulates migration, invasion, EMT in gastric cancer cells. *Clin Exp Pharmacol Physiol* 46: 144-152, 2019.
- Lu J, Guo H, Treekitkarnmongkol W, Li P, Zhang J, Shi B, Ling C, Zhou X, Chen T, Chiao PJ, *et al*: 14-3-3zeta Cooperates with ErbB2 to promote ductal carcinoma in situ progression to invasive breast cancer by inducing epithelial-mesenchymal transition. *Cancer Cell* 16: 195-207, 2009.
- Messaritou G, Grammenoudi S and Skoulakis EM: Dimerization is essential for 14-3-3zeta stability and function in vivo. *J Biol Chem* 285: 1692-1700, 2010.
- Tzivion G, Luo Z and Avruch J: A dimeric 14-3-3 protein is an essential cofactor for Raf kinase activity. *Nature* 394: 88-92, 1998.
- Reddy Chichili VP, Kumar V and Sivaraman J: Linkers in the structural biology of protein-protein interactions. *Protein Sci* 22: 153-167, 2013.
- Mishra R, Gorlov IP, Chao LY, Singh S and Saunders GF: PAX6, paired domain influences sequence recognition by the homeodomain. *J Biol Chem* 277: 49488-49494, 2002.
- Wilson KA, Bär S, Maerz AL, Alison M and Pountourios P: The conserved glycine-rich segment linking the N-terminal fusion peptide to the coiled coil of human T-cell leukemia virus type 1 transmembrane glycoprotein gp21 is a determinant of membrane fusion function. *J Virol* 79: 4533-4539, 2005.
- Nagi AD and Regan L: An inverse correlation between loop length and stability in a four-helix-bundle protein. *Fold Des* 2: 67-75, 1997.
- Kuusinen A, Arvola M and Keinänen K: Molecular dissection of the agonist binding site of an AMPA receptor. *EMBO J* 14: 6327-6332, 1995.
- Wang W, Prosser WW, Chen J, Taremi SS, Le HV, Madison V, Cui X, Thomas A, Cheng KC and Lesburg CA: Construction and characterization of a fully active PXR/SRC-1 tethered protein with increased stability. *Protein Eng Des Sel* 21: 425-433, 2008.
- Mir N, Jayachandran A, Dhungel B, Shrestha R and Steel JC: Epithelial-to-mesenchymal transition: A mediator of sorafenib resistance in advanced hepatocellular carcinoma. *Curr Cancer Drug Targets* 17: 698-706, 2017.
- Ahn HM, Yoo JW, Lee S, Lee HJ, Lee HS and Lee DS: Peroxiredoxin 5 promotes the epithelial-mesenchymal transition in colon cancer. *Biochem Biophys Res Commun* 487: 580-586, 2017.
- Castro NP, Rangel MC, Merchant AS, MacKinnon G, Cuttitta F, Salomon DS and Kim YS: Sulforaphane suppresses the growth of triple-negative breast cancer stem-like cells in vitro and in vivo. *Cancer Prev Res (Phila)* 12: 147-158, 2019.



This work is licensed under a Creative Commons Attribution-NonCommercial-NoDerivatives 4.0 International (CC BY-NC-ND 4.0) License.